

Time-resolved measurement of free carrier absorption, diffusivity, and internal quantum efficiency in silicon

Jet Meitzner,¹ Frederick G. Moore,² Brock M. Tillotson,¹ Stephen D. Kevan,^{1,a)} and Geraldine L. Richmond¹

¹Department of Chemistry, University of Oregon, Eugene, Oregon 97403, USA

²Department of Physics, Whitman College, Walla Walla, Washington 99362, USA

(Received 25 June 2013; accepted 13 August 2013; published online 26 August 2013)

We demonstrate an innovative pump-probe technique for the determination of free carrier absorption, diffusivity, and internal quantum efficiency in Si. The internal quantum efficiencies for excitation by 800 nm, 400 nm, and 267 nm light are found to be 1.00, 1.00, and 1.25, respectively. The free carrier absorption cross section at 1510 nm is determined to be $\sigma_{FCA} = 1.69 \times 10^{-17} \text{ cm}^2$ and an increased value is observed for high carrier concentrations. A model for free carrier diffusion and absorption is used to extract the relationship between σ_{FCA} and carrier concentration.

© 2013 AIP Publishing LLC. [<http://dx.doi.org/10.1063/1.4819447>]

The performance of photovoltaic materials depends predominantly on ultrafast carrier dynamics such as carrier cooling, diffusion, and recombination. In the development of more efficient solar technology, a contactless and nondestructive probe of these dynamics is vital. Indeed, a number of methods (e.g., pump-probe, photoconductivity, two-photon photoemission, photoluminescence) have been developed to study these phenomena.^{1–3} Among them, pump-probe is most attractive due to pulse-width limited time resolution, ease of control over carrier injection level, and access to both bulk and surface phenomena in direct and indirect bandgap materials.^{4–7}

Of particular technological interest is the quantum efficiency of photocarrier generation. In silicon solar cells, photons with energy greater than the bandgap produce free carriers with excess energy (*hot carriers*) that typically relax by carrier-phonon scattering (heat generation) within a few hundred femtoseconds.^{1,2} For photon energies near or exceeding the direct bandgap energy (3.4 eV), carrier-carrier scattering can instead generate a second electron-hole pair through impact ionization, and the internal quantum efficiency (IQE) exceeds unity.^{8,9} This can lead to increased solar cell efficiency, and in fact some researchers seek to engineer 3rd generation photovoltaic materials that will promote impact ionization over heat generation.¹⁰

Herein, an all-optical and nondestructive pump-probe technique is demonstrated for the measurement of free carrier absorption (FCA), diffusivity, and IQE in a bulk semiconductor through detection of both the transmission and reflection of the probe beam. The method relies on the well-known free carrier-induced changes in the reflectivity and absorptivity of a semiconductor, which are well described by the Drude model.¹¹ Accordingly, free carriers absorb infrared (IR) and near-IR radiation with a sensitivity given by the free carrier absorption cross section σ_{FCA} . By quantifying the FCA of a probe beam in the near-IR, the Beer-Lambert

relationship is used to calculate the free carrier sheet concentration (FCSC)

$$N_{\square} = \frac{\ln\left(\frac{I_0}{I}\right)}{\sigma_{FCA}}, \quad (1)$$

where I_0 is the incident probe pulse energy and I is I_0 minus the energy absorbed by free carriers. N_{\square} represents the number of free carriers per unit area of the substrate surface and is equal to the volume carrier concentration (N) integrated through the depth of the sample.

The experimental setup is shown in Fig. 1. An amplified Ti:Sapphire laser (Spectra-Physics Tsunami) produces 800 nm pulses of approximately 110 fs FWHM duration at a repetition rate of 1 kHz, which are split into a pump line and probe line. The pump line can undergo second and third harmonic generation using beta-barium borate (BBO) crystals to produce 400 nm or 267 nm light, respectively. A portion of each pump pulse is collected by detector D3 and used for excitation energy normalization. The probe line undergoes optical parametric amplification to produce 1510 nm, and travels along a delay stage that provides up to 3.5 ns of delay time relative to the pump pulse. Both the transmission and reflection of the probe pulses are detected and normalized using a probe reference detector (D4) to increase the signal to noise ratio.

The samples used in this study are double-side polished $\langle 100 \rangle$ Si wafers of high purity (undoped, $R = 5000\text{--}8000 \ \Omega \text{ cm}$). The wafers are subjected to the RCA standard clean¹² followed by etching in buffered oxide etch (BOE), and finally oxidation in a tube furnace to grow a thermal oxide of approximately 50 nm. The thermal oxide produces a smooth Si/SiO₂ interface¹³ that minimizes surface recombination.

The purpose of monitoring the reflectivity of the probe beam is two-fold. First, the magnitude of $\Delta R/R$ is proportional to total number of free carriers in the effective observation depth of approximately 35 nm ($= \lambda/4\pi|n|$, where n is the complex index of refraction).² Therefore, a measure of reflectivity provides a picture of how the near-surface carrier concentration evolves in time. Second, ΔR is used as a

^{a)} Author to whom correspondence should be addressed. Electronic mail: kevan@uoregon.edu.

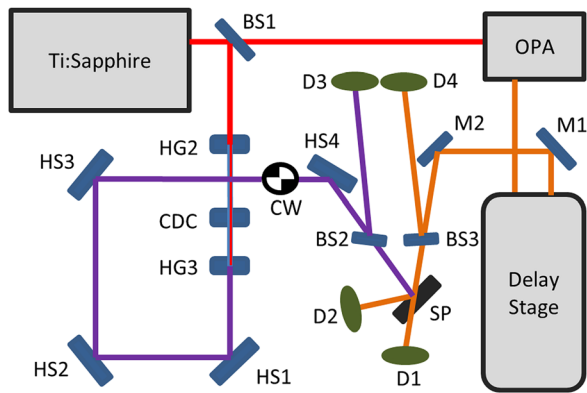


FIG. 1. Experimental setup. BS, beam splitter; OPA, optical parametric amplifier; HG2, 2nd harmonic generation BBO crystal; HG3, 3rd harmonic generation BBO crystal; CDC, calcite delay compensator; HS, harmonic separator; M, mirror; D, detector; SP, sample; CW, chopper wheel.

correction factor when calculating the amount of FCA from ΔT (T is transmission). When the near surface carrier concentration is high, the change in reflectivity can significantly affect the amount of light that is transmitted through the wafer. By monitoring both ΔR and ΔT , an accurate value for FCA is determined.

In order to calculate IQE from the measured FCSC, a careful normalization is performed. The FCSC is normalized by the pump beam photon flux in the probed region, corrected for sample reflectivity. When the pump beam is much larger than the probe beam and the two are well overlapped, this flux is approximately constant over the probed region. In this study, the Gaussian beam width of the pump beam is always at least $7\times$ larger than that of the probe beam. Therefore, the photon flux at the center of the pump beam is

used for the normalization. It is calculated using the total pump pulse energy and spatial profile of the beam (measured using the razor edge method).

σ_{FCA} is the free parameter in the calculation of IQE. Following the normalization described above, the value of σ_{FCA} is assigned a value such that the IQE for carrier generation by 800 nm is equal to unity. This produces $\sigma_{FCA} = 1.69 \times 10^{-17} \text{ cm}^2$, which is the value used with Eq. (1) for analysis of the data presented in Figures 2 and 3. The value of σ_{FCA} is not documented for the probe wavelength of 1510 nm, but the value determined here is in good agreement with literature values when taking into account the well-known λ scaling behavior.^{7,14}

Fig. 2 shows the IQE of carrier generation in Si for each of the excitation wavelengths. At time $t = 0$, the pump pulse promotes electrons from the valence band to the conduction band. These free carriers are generated with a concentration profile that decays exponentially according to the absorption parameter α .⁴ In Si, photons with energy near or exceeding the direct band-gap (3.4 eV) are absorbed very quickly, giving rise to high carrier concentrations ($\leq 2.5 \times 10^{20} \text{ cm}^{-3}$) near the surface of the wafer where light is incident. These carrier concentrations require a more elaborate treatment of N_{\square} than Eq. (1), which assumes a constant value for σ_{FCA} . Indeed, this assumption leads to an apparent decay of IQE in the traces for 400 nm and 267 nm (beginning at 1 ps and ending by 2000 ps). The decay is absent for 800 nm due to the much longer absorption depth and consequently lower carrier concentration. A model for the treatment of σ_{FCA} at high N is discussed below.

Each trace in Fig. 2 flattens by $t = 2000$ ps to a single value of IQE. At this point, the only decay in IQE would be due to interband recombination. The traces appear flat

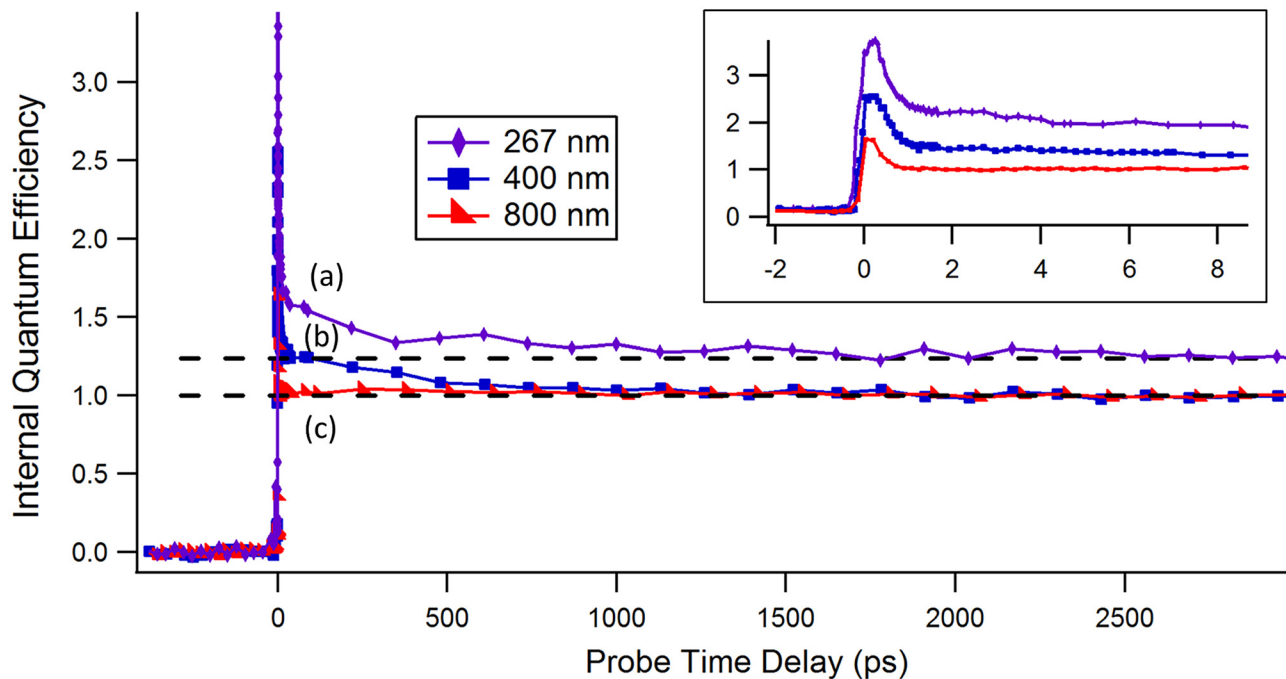


FIG. 2. Internal quantum efficiency for carrier generation in Si at three different excitation wavelengths. Excitation intensities are $94 \mu\text{J}/\text{cm}^2$, $157 \mu\text{J}/\text{cm}^2$, and $77 \mu\text{J}/\text{cm}^2$ for 267 nm, 400 nm, and 800 nm, respectively. The decays in traces (a) and (b) correspond to carrier diffusion from regions of high carrier density to regions of lower carrier density. The IQE is the value at which the traces flatten. The dashed lines are at IQE values of 1.00 and 1.25. The inset is zoomed in around time $t = 0$.

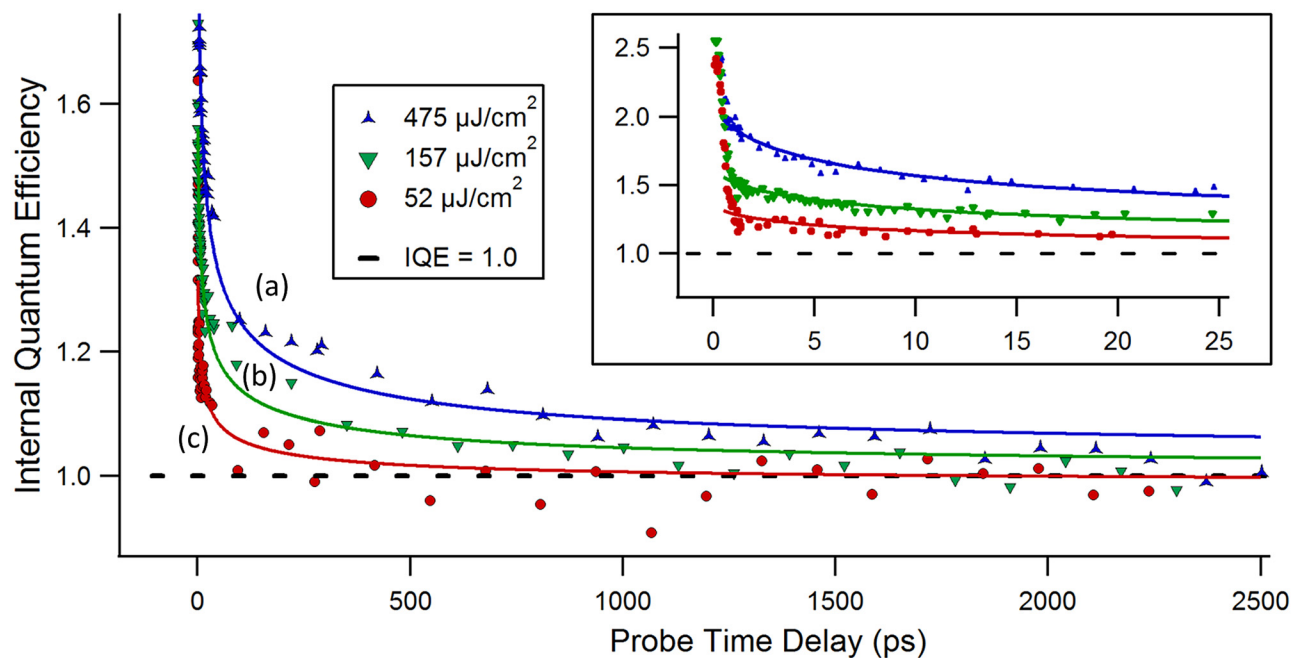


FIG. 3. Excitation intensity dependence of the apparent decay in IQE for 400 nm excitation. Solid lines are fits to the data, where the N dependence of σ_{FCA} is taken into account. The inset is zoomed in after time $t=0$.

because this recombination is slow relative to the timescale of the measurement. Therefore, the IQE values have been extracted as the asymptotic value of each trace at long time (dashed lines). The values of IQE are 1.00, 1.00, and 1.25 for 800 nm, 400 nm, and 267 nm, respectively. Within our preliminary data sets, the range of IQE values extracted from scans under nominally identical experimental conditions is within the range ± 0.02 .

The values of IQE determined here are consistent with those previously obtained by measurements of reflectance and short circuit current on illuminated solar cell devices.⁸ Though there is always some uncertainty in the measurement of reflectivity and calibration of reference detectors, it is well known that the IQEs for 800 nm and 400 nm illumination are equal to unity.¹⁵ For photon energies exceeding 3.25 eV, however, there is some discrepancy in the reported values. In many cases, this is attributed to differences in doping or a free carrier collection efficiency that depends on excitation wavelength, both of which are irrelevant for the contactless technique demonstrated here. In any case, the values of IQE previously reported for 267 nm excitation fall within the range of 1.1–1.3.⁸

The decay of IQE in the 267 nm and 400 nm traces (Fig. 2) is due to a free carrier absorption cross section (σ_{FCA}) that is increased immediately after excitation and decays with time to the constant value of $1.69 \times 10^{-17} \text{ cm}^2$. There are two possible explanations for the increase in σ_{FCA} . One is that the free carrier excess energy is dissipated to the lattice within a few hundred fs of excitation, resulting in an elevated lattice temperature.^{1,2,16} Since σ_{FCA} increases linearly with temperature,¹⁷ this could result in an initially increased value for σ_{FCA} that decays as the lattice equilibrates with room temperature. However, using the approach in Ref. 17 and an estimated maximum lattice temperature increase in 6 K (for trace (b) in Fig. 2), σ_{FCA} is only expected

to increase by $0.02 \times 10^{-17} \text{ cm}^2$. Thus, this explanation cannot account for the observed enhancement in σ_{FCA} of up to a factor of 1.5. The second explanation is that 400 nm and 267 nm lights have short absorption depths of approximately 90 nm and 5 nm, respectively,¹⁸ resulting in high free carrier concentrations near the surface of the sample. It is known that σ_{FCA} increases with carrier concentrations greater than approximately $2 \times 10^{17} \text{ cm}^{-3}$,^{4,19} due to increased rates for carrier-carrier scattering.^{20,21,27} With initial ($t=0$) near-surface carrier concentrations of $2.5 \times 10^{20} \text{ cm}^{-3}$ and $3.5 \times 10^{19} \text{ cm}^{-3}$ for traces (a) and (b) in Fig. 2, respectively, this should result in an initially increased value for σ_{FCA} that decays as carriers diffuse into the bulk.

To account for consequences of these two effects (carrier diffusion and the dependence of σ_{FCA} on N) in determining IQE, we begin with diffusion. The initial distribution of photocarriers is exponential, and we assume that it evolves in time according to Fick's Law. This one-dimensional Fick's Law diffusion problem (with an initial exponential distribution) has been solved analytically²² and gives $N(z,t)$. Knowing the absorbed excitation photon flux and absorption depth, the only remaining parameter is the carrier diffusivity which we take to be $20 \text{ cm}^2/\text{s}$.^{23,24}

From Isenberg and Warta,²⁵ the shape of the σ_{FCA} versus N relationship is clearly sigmoidal in $\log(N)$ (Fig. 4). In modeling our IQE curves, we adopt this form but allow the sigmoid parameters to vary as we perform a non-linear least squares global fit of the data in Fig. 3. The fitting algorithm is derived from the differential form of the Beer-Lambert relationship and integrated over 10 absorption depths (of the pump beam):

$$\ln\left(\frac{I_o}{I}\right) = \int_0^{10z} N(z,t)\sigma(z,t)dz. \quad (2)$$

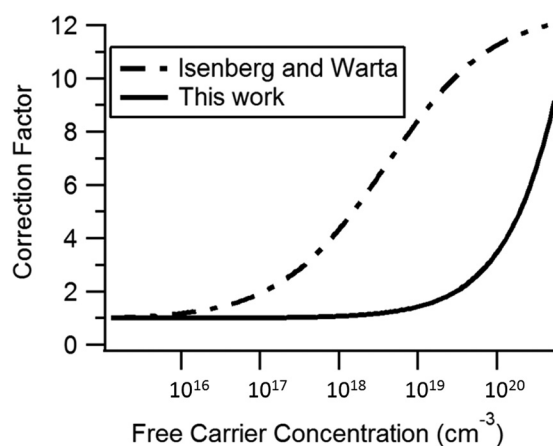


FIG. 4. Correction factor for σ_{FCA} relative to the value at $N=10^{16}\text{ cm}^{-3}$. This work applies to FCA in photo-excited Si, while the curve from Isenberg and Warta applies to FCA in doped Si. Reproduced with permission from J. Isenberg and W. Warta, *Appl. Phys. Lett.* **84**(13), 2265 (2004). Copyright 2004 American Institute of Physics.

This analysis has essentially asked the question: Is our determination of IQE consistent with a model where σ_{FCA} varies with depth and time because of its dependence on $N(z,t)$? The answer, judging from Figure 3, is certainly yes. At times greater than 1 ps, the solid lines of our model fits are in very good agreement with the experimental data.

Fig. 3 shows the excitation intensity dependence of IQE for 400 nm excitation. For clarity, we have truncated the data on the rising edge of the initial peak ($t < 0$). The inset shows that the magnitude of the decay increases monotonically with excitation intensity, as is predicted by the N dependence of σ_{FCA} discussed above. Furthermore, each data set asymptotically approaches the same IQE value of 1.00, which verifies that the decay is not due to recombination. The fits for (a) and (b) slightly overestimate the IQE at long times, which may be due to carrier diffusivity that increases with decreasing carrier concentration,^{24,26} whereas our model assumes a constant diffusivity.

Our determination of σ_{FCA} enhancement versus N for photocarriers is shown in Fig. 4, along with Isenberg and Warta whose work applies to FCA in doped Si. The lower enhancement factor determined here can be explained by the difference between samples where free carriers are produced by photo-excitation versus those where free carriers are produced by doping. The enhancement of σ_{FCA} in doped samples is largely due to carrier-lattice scattering and is well predicted by the change in carrier mobility.^{21,25} This effect causes an enhancement in σ_{FCA} beginning at carrier concentrations of approximately $1 \times 10^{16}\text{ cm}^{-3}$.²⁵ In contrast, the enhancement of σ_{FCA} in photo-excited samples occurs due to carrier-carrier scattering, and arises only for concentrations $> 2 \times 10^{17}\text{ cm}^{-3}$.^{4,7,19,21,27} Thus, it is not surprising that the observed enhancement in σ_{FCA} begins at approximately 10^{18} cm^{-3} .

Free carrier diffusion into the bulk is verified by a plot of $\Delta R/R$ versus probe time delay (data not shown). The magnitude of $\Delta R/R$ is proportional to the total number of free carriers within approximately 35 nm of the Si surface, and the decay corresponds to diffusion of carriers into the

bulk.^{6,28} The timescale of the decay in $\Delta R/R$ and the decay in IQE are nearly equivalent, giving support to the conclusion that the decay in IQE is due to carrier diffusion.

In conclusion, a contactless and nondestructive method has been demonstrated for the observation of free carrier absorption, diffusivity, and IQE in semiconductors. By monitoring both the reflection and transmission of the probe beam and normalizing by absorbed excitation photon flux, the IQE of carrier generation in Si has been measured for three different excitation wavelengths. Using this technique on bulk semiconductors, the IQE along with an observation of ultrafast carrier dynamics is available within the same experiment. Work in progress applies this technique to more complex photovoltaic materials to explore the possibility of heterojunction assisted impact ionization in unbiased materials.

The authors would like to thank Dr. Larry Scatena and Dr. Pat Blower for many informative discussions and insights, and the National Science Foundation (Award No. DMS-1035513) for support of this research.

- ¹T. Ichibayashi, S. Tanaka, J. Kanasaki, K. Tanimura, and T. Fauster, *Phys. Rev. B* **84**(23), 235210 (2011).
- ²A. Sabbah and D. Riffe, *Phys. Rev. B* **66**(16), 165217 (2002).
- ³P. R. Smith, *Appl. Phys. Lett.* **38**(1), 47 (1981); M. Dovrat, Y. Goshen, J. Jedrzejewski, I. Balberg, and A. Sa'ar, *Phys. Rev. B* **69**(15), 155311 (2004).
- ⁴V. Grivickas, A. Galeckas, V. Bikbajevs, J. Linnros, and J. A. Tellefsen, *Thin Solid Films* **364**(1–2), 181 (2000).
- ⁵Z. G. Ling and P. K. Ajmera, *J. Appl. Phys.* **69**(1), 519 (1991).
- ⁶T. Tanaka, A. Harata, and T. Sawada, *J. Appl. Phys.* **82**(8), 4033 (1997).
- ⁷J. Linnros, *J. Appl. Phys.* **84**(1), 275 (1998).
- ⁸S. Kolodinski, J. H. Werner, T. Wittchen, and H. J. Queisser, *Appl. Phys. Lett.* **63**(17), 2405 (1993); M. Wolf, R. Brendel, J. H. Werner, and H. J. Queisser, *J. Appl. Phys.* **83**(8), 4213 (1998).
- ⁹J. Tauc, *J. Phys. Chem. Solids* **8**(0), 219 (1959); V. S. Vavilov, *ibid.* **8**(0), 223 (1959).
- ¹⁰D. Westley Miller, P. Hugger, J. Meitzner, C. W. Warren, A. Rockett, S. Kevan, and J. David Cohen, "A contactless photoconductance technique for the identification of impact ionization," IEEE PVSC (submitted).
- ¹¹J. Kim, *J. Korean Phys. Soc.* **55**(2), 512 (2009); M. I. Gallant and H. M. Vandriel, *Phys. Rev. B* **26**(4), 2133 (1982).
- ¹²W. Kern, *J. Electrochem. Soc.* **137**(6), 1887 (1990).
- ¹³K. A. Reinhardt and W. Kern, *Handbook of Silicon Wafer Cleaning Technology*, 2nd ed. (William Andrew, Inc., Norwich, NY, 2008), p. 558.
- ¹⁴W. B. Gauster, *J. Appl. Phys.* **41**(9), 3850 (1970); H. Rogne, P. J. Timans, and H. Ahmed, *Appl. Phys. Lett.* **69**(15), 2190 (1996); W. Spitzer and H. Fan, *Phys. Rev.* **108**(2), 268 (1957).
- ¹⁵F. J. Wilkinson, A. J. D. Farmer, and J. Geist, *J. Appl. Phys.* **54**(2), 1172 (1983); J. Geist and E. F. Zalewski, *Appl. Phys. Lett.* **35**(7), 503 (1979).
- ¹⁶F. E. Doany and D. Grischkowsky, *Appl. Phys. Lett.* **52**(1), 36 (1988).
- ¹⁷K. G. Svantesson and N. G. Nilsson, *J. Phys. C* **12**(18), 3837 (1979).
- ¹⁸G. E. Jellison, *Appl. Phys. Lett.* **41**(2), 180 (1982).
- ¹⁹V. Grivickas, *Solid State Commun.* **108**(8), 561 (1998).
- ²⁰C. M. Horwitz and R. M. Swanson, *Solid-State Electron.* **23**(12), 1191 (1980).
- ²¹V. Grivickas, M. Willander, and J. Vaitkus, *Solid-State Electron.* **27**(6), 565 (1984).
- ²²G. J. Willems and H. E. Maes, *J. Appl. Phys.* **73**(7), 3256 (1993).
- ²³C. M. Li, T. Sjodin, Z. C. Ying, and H. L. Dai, *Appl. Surf. Sci.* **104**, 57 (1996).
- ²⁴M. Rosling, H. Bleichner, P. Jonsson, and E. Nordlander, *J. Appl. Phys.* **76**(5), 2855 (1994).
- ²⁵J. Isenberg and W. Warta, *Appl. Phys. Lett.* **84**(13), 2265 (2004).
- ²⁶M. Rosling, H. Bleichner, M. Lundqvist, and E. Nordlander, *Solid-State Electron.* **35**(9), 1223 (1992); C. M. Li, T. Sjodin, and H. L. Dai, *Phys. Rev. B* **56**(23), 15252 (1997).
- ²⁷B. E. Sernelius, *Phys. Rev. B* **39**(15), 10825 (1989).
- ²⁸A. J. Sabbah and D. M. Riffe, *J. Appl. Phys.* **88**(11), 6954 (2000).